

## Supporting information

### **Nanoparticles can modulate network topological defects during multimodal elastomer formation**

Kishore Kumar Sriramoju<sup>a</sup>, \*Sangram K Rath<sup>b</sup>, Debargha Sarkar<sup>a</sup>, Kathi Sudarshan<sup>b</sup>,  
Pradeep K Pujari<sup>b</sup> and \*G. Harikrishnan<sup>a</sup>

*<sup>a</sup>Department of Chemical Engineering, Indian Institute of Technology Kharagpur,  
West Bengal, 721302, India*

*<sup>b</sup>Bhabha Atomic Research Centre, Mumbai, 400085, India*

*<sup>c</sup>Naval Materials Research Laboratory, Ambernath, Maharashtra, 421506, India*

\* Corresponding authors: Sangram K Rath: sangramkrath@gmail.com; G. Harikrishnan: hari@iitkgp.ac.in; Tel: +913222283928; Fax: +913222255303

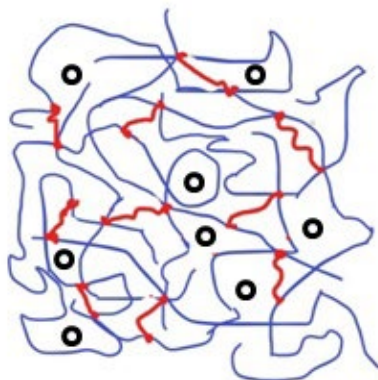


Figure S1. Representational sketch of bimodal network in an elastomer<sup>1</sup>. Long chains (blue coloured) are end-linked to short chains (red coloured). The circles show molecular free space within the network.

## Materials and Methods

### *Materials*

Long (number average molecular weight,  $M_n=18952$  g/mol, polydispersity index=1.9, GE Bayer Silicones) and short chains ( $M_n=4323$  g/mol, polydispersity index=1.8, Dow corning) of hydroxyl-terminated poly(dimethyl siloxane) are used. Unimodal networks are prepared separately from these chains. For bimodal networks, they are mixed at a weight ratio of 80:20. A cross-linker (tetraethoxyorthosilane (TEOS, Sigma-Aldrich)) and a catalyst (Dibutyltin dilaurate (DBTDL, Sigma-Aldrich)) were used for cross-linking reaction. Organically modified layered montmorillonite (Cloisite 10A, BYK Additives, USA) was used as the NP. The organic modifier used is a quaternary ammonium salt of dimethyl benzyl hydrogenated tallow. A single layer of montmorillonite is approximately 1 nm thick and 100-150 nm in lateral dimensions. The interlamellar distance between clay sheets are reported by the manufacturer as 1.92 nm<sup>2</sup>.

### ***Preparation of NP-oligomer dispersions***

The NP is initially blended with a mixture of long and short chain precursors using a mechanical stirrer (RQ 122, Remi Motors) at a speed of 3000 rpm. This is followed by very high shear dispersion using a digital pigment Muller (92-NM, LLOYDS). A picture of the equipment, its specifications, and a schematic of shearing disks are given in Figure S2. The initially blended suspension is placed at the centre of the disks. The upper plate is stationary and the lower plate rotates. A rotational speed of 50 rpm was used which transfers a substantial force of 60 kgf to the suspension kept between the disks. The rotation was conducted for 30 minutes. After this, the spread suspension is again gathered at the centre of the lower plate using a spatula. The rotation is again repeated. A total of three rotations were conducted. The approximate shear applied on each prepolymer-NP blend is estimated and is tabulated in Table S1.

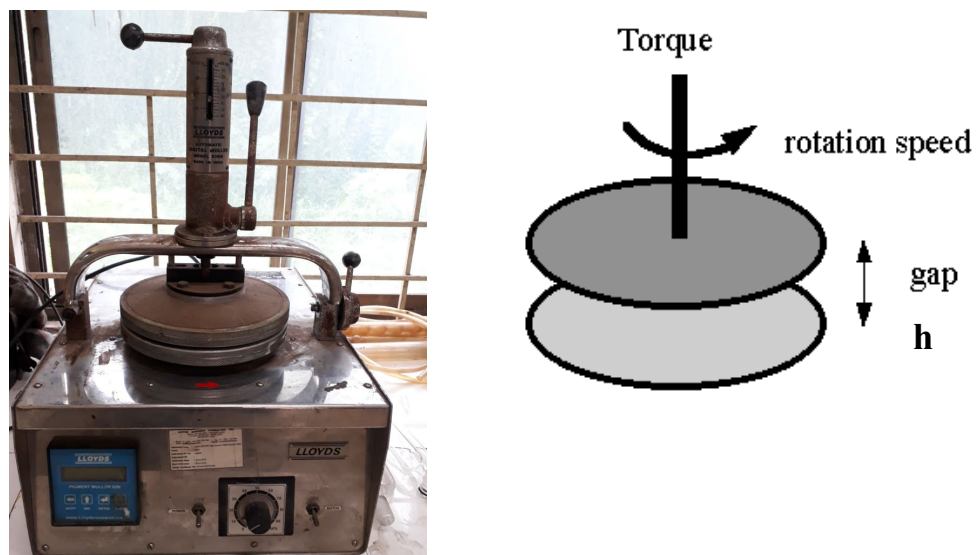


Figure S2. Picture of high shear Muller and schematic of rotating disks

System specifications<sup>3</sup>:

Power  $P = 0.37$  kW, Rotation speed  $\omega = 50$  rpm, Torque ( $T$ ) =  $P/\omega = 71.4$  N-m, Gap between plates  $h = 0.2$  mm. In the shear estimation done in the main article, the rotating direction is considered as  $\theta$ , the radial direction of the disk as  $r$  and the remaining direction  $z$ . The estimation of maximum shear stress applied on dispersions are estimated as shown below.

The two parallel disks (Figure S2) shear the fluid in between them by a torque  $T$ .

$$\text{Shear rate } \dot{\gamma} = \frac{dV_{\theta}}{dr} \text{ (assumptions } V_z=V_r=0 \text{ and no slip)}$$

for  $h \ll D$ ,  $V_{\theta}$  can be approximated to be linearly varying with  $r$ , for one plate rotating at an angular frequency  $\omega$  with  $v_{\theta} = 0$  for the stationary plate<sup>4</sup>. The linearly approximated shear rate is  $\dot{\gamma} = \frac{\omega r}{h}$ . The total torque acting on the fluid between the

discs  $T = \int_0^R r \cdot \tau \cdot 2\pi r dr$ . Substituting  $r$  in above equation

$$T = \frac{2\pi h^3}{\omega^3} \int_0^{\dot{\gamma}R} \mu_{app}(\dot{\gamma}) \cdot \dot{\gamma}^3 \cdot d\dot{\gamma} \quad (1)$$

the boundary conditions are;  $T=0$  at  $r=0$  and  $T=T$  at  $r=R$

$$\tau_R = \frac{3T}{2\pi R^3} + \frac{T}{2\pi R^3} \frac{\dot{\gamma}R}{T} \cdot \frac{dT}{d\dot{\gamma}R} \quad (2)$$

Substituting  $\frac{dT}{d\dot{\gamma}R}$  and using  $\dot{\gamma}_R = \frac{\omega R}{h}$

$$\tau_{\max} = \frac{3T}{2\pi R^3} + \dot{\gamma}_R \cdot \mu_{app}(\dot{\gamma}_R) \quad (3)$$

Substituting values of respective parameters (refer supporting information)

$$\tau_{\max} = 39.8 \times 10^3 + 2481 \mu_{app}(\dot{\gamma}_R) \quad (4)$$


---

$\mu_{app}(\dot{\gamma}_R)$  is calculated from steady shear diagrams (Figure 1, main article) of dispersions. The estimation of max applied shear at each particle concentration is tabulated in Table S1 below.

Table S1. Estimated maximum shear stress applied by the high shear equipment on prepolymer-NP dispersions

Dispersion	$\mu_{app}(\dot{\gamma}_R)$ (Pa.s)	$\tau_{max}$ (KPa)
C5	2.8	46.7
C10	3.9	49.5
C20	10.9	66.8

### ***Elastomer preparation***

To the above binary mixture (a typical composition of the suspension would be 10.8 g of long chain precursor, 2.7 g of short chain precursor and different concentrations of particles), 0.32 g of cross-linker, and 0.5 g of catalyst were added. The mixture was poured into a Teflon mould of dimensions  $10 \times 10 \times 0.5 \text{ cm}^3$ . The mould was kept at room temperature and the mixture was allowed to cure for 7 days. The networks were collected as free-standing films. Pure bimodal networks were prepared without particle addition. Pure unimodal long and short chain networks are also synthesized in the same way.

### ***State of NP dispersion in oligomers***

A Rheometer (Anton Paar MCR 301, Austria) having a parallel plate assembly (PP50-SN24598) was used. Samples were placed between parallel plates having a gap of 0.2 mm. The shear rate was varied (under rotational shear) between 0.01 to  $1000 \text{ s}^{-1}$ . Since the suspension with the highest mass fraction of particles showed highly shear

thinning behaviour, an additional oscillatory shear experiment was performed to assess the state of particle dispersion. This is done by a frequency sweep test performed within the linear viscoelastic regime. The critical strain that defines the linear viscoelastic regime is estimated by a strain sweep experiment. All rheological measurements were conducted at a constant temperature of 27<sup>0</sup> C, maintained by a Peltier system attached to the Rheometer.

### ***Sol-fraction and elastomer density***

A sheet of 1 x 2 x 0.5 cm<sup>3</sup> in dimensions is weighed ( $W_i$ ) using a high precision electronic balance (Mettler Toledo, XS205). This sample is allowed to swell in Benzene for 2 days at 27<sup>0</sup> C. After 2 days, the swollen sample is again weighed ( $W_f$ ). Then the sample is kept in a dryer at a temperature of 60<sup>0</sup> C for 1 day. The sample is again weighed ( $W_d$ ). The fractional swelling is given by  $(W_f - W_i) / W_i$ . The sol-fraction is  $(W_i - W_d) / W_d$ . The densities of networks were measured using Methanol. The details of the experimental procedure are given elsewhere<sup>5</sup>. The samples were initially weighed in air ( $W_a$ ) followed by weighing ( $W_s$ ) in Methanol. Network density =  $W_a \rho_s / (W_a - W_s)$ , where  $\rho_s$  is the specific gravity of Methanol.

### ***State of NP dispersion in elastomer***

The state of dispersion of particles in the network was examined using a transmission electron microscope (Philips CM12) with an accelerating voltage of 80 kV. Ultra-microtome (Leica EM UC7) was used to prepare thin samples for imaging. The ultra-microtome consists of a cooling chamber at a working temperature of -135<sup>0</sup> C with liquid N<sub>2</sub>. The knife holder includes two glass knives up to 10 mm thickness and allows independent adjustment of clearance angle from 0<sup>0</sup> to 9<sup>0</sup>. The knife is used to cut ultra-thin sections of frozen specimens. The sections are of approximately 70-100 nm thickness and were directly mounted onto TEM copper grids.

### *Topological defects*

Positron annihilation lifetime spectroscopy (PALS) was carried out at room temperature, using a fast-fast coincidence spectrometer. The time resolution of the positron lifetime spectrometer measured for gamma-rays of  $^{60}\text{Co}$  was 265 ps. A 20  $\mu\text{Ci}$   $^{22}\text{Na}$  encapsulated in 8-micron polyimide was sandwiched between two pieces of the same sample. The total area under each lifetime spectra was about  $10^6$  counts. The lifetime spectra were analysed for distribution of lifetimes using Laplace inversion-based program CONTIN<sup>6</sup>.

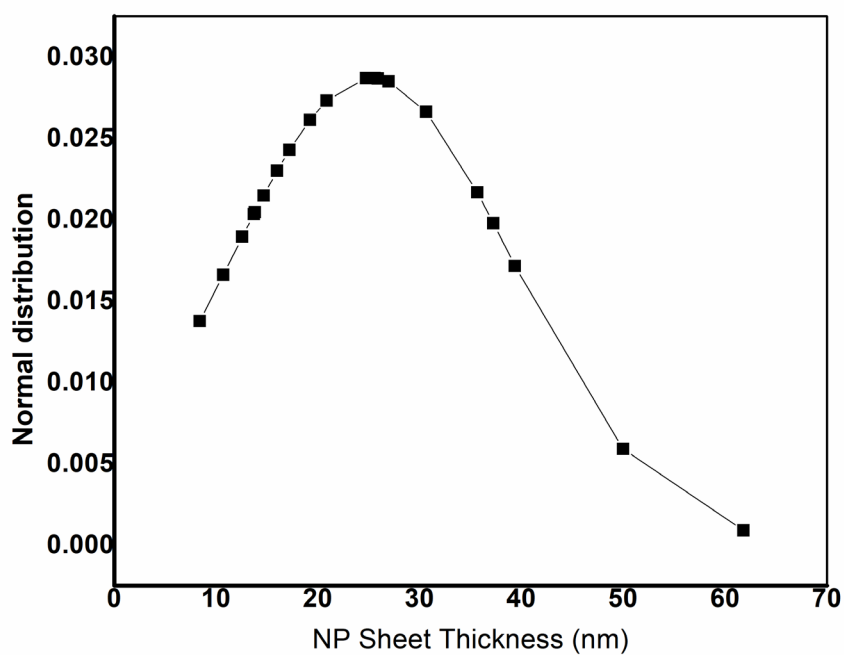


Figure S3. Normal distribution of NP plate thickness extracted from TEM images.

Table S2: Full positron lifetime data

<b>Elastomer</b>	<b><math>\tau_1</math> (ps)</b>	<b><math>I_1</math> (%)</b>	<b><math>\tau_2</math> (ps)</b>	<b><math>I_2</math> (%)</b>	<b><math>\tau_3</math> (ns)</b>	<b><math>I_3</math> (%)</b>	<b><math>\tau_4</math> (ns)</b>	<b><math>I_4</math> (%)</b>
Pure bimodal	141 ± 2	20.5 ± 1.0	357 ± 18	30.8 ± 2.3	0.94 ± 0.10	7.2 ± 2.5	3.39 ± 0.07	41.5 ± 2.7
Bimodal-C5	142 ± 2	17.3 ± 1.1	342 ± 9	36.8 ± 1.1	1.03 ± 0.01	8.1 ± 1.1	3.40 ± 0.01	37.7 ± 0.7
Bimodal-C10	140 ± 2	15.5 ± 1.0	340 ± 5	44.8 ± 1.0	1.00 ± 0.01	7.7 ± 1.1	3.35 ± 0.01	31.9 ± 0.5
Bimodal-C20	172 ± 23	15.1 ± 3.0	343 ± 8	45.5 ± 2.4	0.87 ± 0.09	7.6 ± 2.8	3.35 ± 0.08	31.7 ± 0.6
Unimodal short	189 ± 7	27.1 ± 1.5	450 ± 2	22.0 ± 1.8	1.51 ± 0.32	7.3 ± 1.7	3.52 ± 0.07	43.6 ± 2.1
Unimodal long	145 ± 2	19.3 ± 1.0	344 ± 6	26.8 ± 1.1	1.00 ± 0.01	9.7 ± 1.0	3.41 ± 0.02	44.2 ± 0.4



Table S3. Peak area, centre position, FWHM and peak height estimated from probability distribution, representing free volume distribution and network heterogeneity

Elastomer	Peak-1				Peak-2			
	Area	Centre position ( $\overset{\circ}{\text{Å}}$ )	FWHM ( $\overset{\circ}{\text{Å}}$ )	Height	Area	Centre position ( $\overset{\circ}{\text{Å}}$ )	FWHM ( $\overset{\circ}{\text{Å}}$ )	Height
Unimodal short	0.10	2.37	0.39	0.25	0.62	4.01	0.61	0.94
Unimodal long	0.15	1.65	0.32	0.43	0.63	3.96	0.45	1.30
Pure bimodal	0.10	1.54	0.39	0.25	0.55	3.99	0.77	0.66
Bimodal-C5	0.12	1.71	0.33	0.34	0.52	3.95	0.49	0.99
Bimodal-C10	0.11	1.65	0.29	0.36	0.44	3.92	0.45	0.92
Bimodal-C20	0.11	1.42	0.37	0.27	0.42	3.91	0.59	0.66

---

## References

1. J. E. Mark, Elastomeric Networks with Bimodal Chain-Length Distributions, *Acc. Chem. Res.* 27, 271(1994).
2. <http://www.lookpolymers.com/pdf/BYK-Cloisite-10A-Nanoclay.pdf> (retrieved on 2 February 2022).
3. <https://www.lloydsresearch.com/pdf/Muller.pdf> (retrieved on 2 February 2022).
4. U. Yilmazer, D. M. Kalyon, Slip effects in capillary and parallel disk torsional flows of highly filled suspensions, *J. Rheol.* 33(81),1197 (1989).
5. S. K. Rath, S. K. Sharma, K. Sudarshan, J. G. Chavan, T. U. Patro, P. K. Pujari., Subnanoscopic inhomogeneities in model end-linked PDMS networks probed by positron annihilation lifetime spectroscopy and their effects on thermomechanical properties, *Polymer* 101, 358 (2016).
6. R. B. Gregory, Y. Zhu, *Nuclear Instruments and Methods in Physics Research Section A: Accelerators, Spectrometers, Detectors and Associated Equipment*, *Nucl. Instrum. Methods Phys Res. A* 290, 172 (1990).